Detector R& D for future Neutrino Experiments with the NUMI Beamline

by Future Neutrino Experiments Study Groupies
Asterisks means those persons have agreed to serve...

Contents

I Introduction **2**

II NUMI Off Axis Neutrino Spectra **3**

III Theoretical Motivations **3**

IV Detector Issues and Comparison **7**
A Detector Requirements for θ_{13} . . . 7
1 Neutral Current Rejection in a superbeam . . . 7
2 Intrinsic ν_e Rejection in a superbeam . . . 7
3 Charge identification in a neutrino factory . . . 7
B Operation at the Surface . . . 7
C Expandability . . . 7
D Cost comparisons . . . 7
E Fiducial vs Total Mass . . . 7

V Total Absorption Detectors **7**
A Liquid Argon Detectors . . . 7
B R& D Issues for Liquid Argon Detectors . . . 8
C Water Cherenkov Detectors . . . 8
D R& D Issues for Water Cherenkov Detectors . . . 8
E Water Rich Detectors . . . 8
F R& D Issues for RICH Detectors . . . 8
G KamLAND-like Detectors . . . 8
H R& D Issues for KamLAND-like Detectors . . . 8

VI Sampling Detectors **8**
A Absorber Issues . . . 8
1 steel . . . 8
2 plastic . . . 8
3 water . . . 8
4 cheap low Z material . . . 8
B Solid Scintillator Detectors . . . 8
C R& D Issues for Solid Scintillator Detectors . . . 9

D Liquid Scintillator Detectors . . . 9
E R& D Issues for Liquid Scintillator Detectors . . . 9
F RPC/gas Detectors . . . 9
G R& D Issues for RPC/gas Detectors . . . 9
H Emulsion Detectors . . . 9
I R& D Issues for Emulsion Detectors . . . 9

VII Other R& D Issues 9
A cross sections . . . 9
B pion yields . . . 9
C targetry . . . 9
1 What survives one spill ? . . . 10
2 Target life-time . . . 13
3 Temperature buildup . . . 13
4 Conclusions . . . 14
D Proton Intensity . . . 14

VIII Summary and Conclusions 14

I. INTRODUCTION

Although we as a field have been trying to detect neutrinos for a very long time, the diferent techniques we use are highly constrained by the fact that neutrinos are so very weakly interacting. As an example, consider the historic first and the most recent reactor neutrino detector: Reines and Cowan used 17 tons of liquid scintillator instrumented with phototubes to see the neutrinos from the XXX reactor, and KAMLAND is using 1000 tons of liqiud scintillator instrumented with phototubes to see neutrinos from reactors located all over Japan. Of course the light collectors have improved and expanded, the timing, electronics, and data acquisition has improved, but the fundamental technique for studying reactor neutrinos has not changed.

Just as the topology of neutrino interactions changes dramatically as the neutrino energy increases, so too does the detector technology. At the high energy limit (above a few GeV), neutrinos simply break apart the nucleus and one can measure the incoming neutrino energy from a charged current interaction by calorimetric sampling measurements of the final state particles, which are classified as either the outgoing lepton, or the "hadronic shower". Again, the MINOS detector today is not fundamentally different from the E1A experiment at Fermilab, which measured neutrino interactions calorimetrically with mineral oil-based scintillator and spark chambers, followed by an iron spectrometer. MINOS combines the spectrometer and calorimeter functions, but the detector concept has not changed.

What we have learned in the past many years of neutrino experimentation is that different detectors are suitable for different energy regimes. In this document we will discuss detectors which are being considered for use in the 1-3 GeV regime, in other words, the regime between the two extremes described above. This regime is suitable for experiments which are off the

axis of the NUMI beamline, which are very well-positioned to take the next steps in neutrino oscillation physics.

II. NUMI OFF AXIS NEUTRINO SPECTRA

The NUMI beamline is designed to produce relatively wide-band neutrino beams of peak energy ranging anywhere between 3.5 and 14GeV. Its focusing system consists of two horns, which, depending on their relative spacing and their spacing from the NUMI target, can focus pions of varying momentum ranges. Because muon neutrinos come predominantly from 2-body pion (and a few kaon) decays, the neutrino energy at a far detector, E_ν, is determined simply by geometry and kinematics:

$$E_\nu = \gamma m_h * \frac{m_h^2 - m_\mu^2}{m_h^2} * \frac{1}{1+\theta^2\gamma^2}$$

where γ is simply the parent meson's relativistic boost, m_h is the parent meson's mass, and θ (assumed to be $<< 1$) is the angle in radians between the detector and the parent meson's direction of flight.

For a perfectly-focused beam, and a detector at $\theta = 0$, the neutrino energy is simply proportional to the parent meson's energy. However for a detector at a non-zero angle, the energy is considerably less, and no longer proportional. For detectors which are 0 and 15mrad from the beamline axis, the neutrino spectra which can be produced by the NUMI beamline is shown in figure XXX.

While a wide-band beam is optimal for precise measurements of the mixing angle and mass splitting separately, in order to maximize the reach for $\nu_\mu \rightarrow \nu_e$ one will be more concerned with backgrounds, and because of this a narrow band beam would be preferable. Notice also that the actual flux of neutrinos at 2GeV is higher for an off-axis beam, which means the average oscillation probability ($\sin^2(\Delta m^2_{32} L/2E)$ for that beam is in fact higher as well.

III. THEORETICAL MOTIVATIONS

In a modern theoretical context, one generally expects nonzero neutrino masses and associated lepton mixing. There is currently strong experimental evidence for neutrino masses and mixing. One source of this evidence is from solar neutrino experiments, most recently, SuperKamiokande and SNO [1]. This data can be fit by oscillations of the solar ν_e's into ν_μ and ν_τ, with the relevant $\Delta m^2_{21} = m(\nu_2)^2 - m(\nu_1)^2 \simeq 5 \times 10^{-5}$ eV^2 and mixing angle $\tan^2\theta_{12} \simeq 0.4$ [2]. Strong evidence also comes from atmospheric neutrino experiments, especially SuperKamiokande [3], with confirming results from Soudan-2 and MACRO. The atmospheric neutrino data can be fit by $\nu_\mu \rightarrow \nu_\tau$ oscillations with $|\Delta m^2_{32}| \simeq 2.5 \times 10^{-3}$ eV^2 and maximal mixing, $\sin^2 2\theta_{23} = 1$ [3]. A pioneering long-baseline accelerator neutrino oscillation experiment, K2K [4], has obtained data consistent with SuperKamiokande results. The sum of data from these experiments can be explained in terms of oscillations involving

the three neutrinos ν_e, ν_μ, and ν_τ, members of electroweak doublets. This data excludes light electroweak-singlet ("sterile") neutrinos as playing a large role in the oscillations. There is also a reported observation of $\bar{\nu}_\mu \to \bar{\nu}_e$ oscillations by the LSND experiment [6], which is not confirmed, but also not completely excluded, by the similar KARMEN experiment [7]. The LSND claim will be tested by the MiniBooNE experiment at Fermilab [8], which is currently in an early commissioning phase, and expects to present definitive results in about two years.

In the standard model generalized to include neutrino masses and without mixing with light sterile neutrinos, the weak leptonic charged current has the form $J_\lambda = \bar{\nu}_L U \gamma_\lambda \ell_L$, where the vector of neutrino mass eigenstates is $\nu = (\nu_1, \nu_2, \nu_3)$ and the analogous vector of charged lepton mass eigenstates is $\ell = (e, \mu, \tau)$. The 3×3 unitary lepton mixing matrix U depends on three Euler rotation angles θ_{12}, θ_{13}, and θ_{23}, and a phase δ, all of which can be probed in neutrino oscillation experiments, and (potentially) two other Majorana phases which cannot be directly tested. For $|\Delta m^2_{23}| \gg \Delta m^2_{12}$ and ignoring matter effects, the probability for $\nu_\mu \to \nu_\tau$ is

$$P(\nu_\mu \to \nu_\tau) = \sin^2(2\theta_{23}) \cos^4 \theta_{13} \sin^2 \phi_{32} \tag{3.1}$$

where

$$\phi_{ij} = \frac{\Delta m^2_{ij} L}{4E} \tag{3.2}$$

and $\Delta m^2_{ij} = m(\nu_i)^2 - m(\nu_j)^2$. Since the best fit to the SuperKamikande data has maximal mixing, it follows that $\theta_{23} \simeq \pi/4$ and $\theta_{13} \ll 1$. The latter constraint also arises from the CHOOZ reactor antineutrino experiment [5]. The CHOOZ limit is dependent on the input value used for $|\Delta m^2_{32}|$; for the current central value 2.5×10^{-3} eV^2, this is $\sin^2(2\theta_{13}) < 0.11$, while for $|\Delta m^2_{32}| = 2.0 \times 10^{-3}$ eV^2, it is $\sin^2(2\theta_{13}) < 0.18$ [5].

The evidence for neutrino oscillations, and hence neutrino masses and lepton mixing, constitutes the first confirmed indication for physics beyond the standard model since its establishment more than 25 years ago. This has led to an intensive program of experimentation to explore further this physics. Fermilab is strongly positioned in this program with the MiniBooNE experiment now beginning data-taking [8] and the MINOS experiment under construction [9]. MINOS will use a neutrino beam with an energy of order a few GeV, traversing a pathlength of $L = 732$ km, from Fermilab to Soudan, MN and will perform several very important measurements, including (i) ν_μ charged-current event rate and energy spectrum, which will check the results of the atmospheric neutrino experiments and is expected to measure the values of $\sin^2 2\theta_{23}$ and $|\Delta m^2_{32}|$ to about 10 %, and (ii) the ν_μ neutral-current event rate, which will provide a cross-check on the oscillation fit and put constraints on the involvement of light electroweak-singlet neutrinos in the oscillations. The proton beam intensity is anticipated to be between about 0.25 MW and 0.4 MW. The above sensitivities are based on 10 kton-yrs of data, i.e. about 2 yrs with the 5 kton MINOS detector. The MINOS program is nicely complementary to the CERN-Gran Sasso neutrino program, in which the OPERA experiment is designed to explicitly detect τ appearance [10]. In Japan, the rebuilding of SuperKamiokande is underway, and the K2K experiment is expected to begin running again in late 2002. Beyond this, there is an ambitious long-baseline neutrino

oscillation experiment that plans to use an intense ν_μ beam from the Japan Hadron Facility JHF which will traverse a distance of 295 km to the fully rebuilt SuperKamiokande detector [11] (JHF-SK). This beam will have an energy $\lesssim 1$ GeV and be produced by an intense 0.77 MW proton beam at JHF. The JHF-SK experimental program envisions measurements of ν_μ disappearance to get high-precision determinations of $|\Delta m^2_{32}|$ and $\sin^2 2\theta_{23}$ and a search for $\nu_\mu \to \nu_e$ oscillations down to a sensitivity of $\sin^2\theta_{13}$ of 0.0015 [11] (see further below). Assuming requisite funding for beamlines, etc. the JHF-SK experiment expects to start commissioning in 2007-2008. Later running with a $\bar{\nu}_\mu$ beam is also planned, and consideration has been given to a second phase of the JHF-Kamioka neutrino program involving the construction of a very large 1 Mton water Cherenkov detector, HyperKamiokande.

Given the large investment that the U.S. high-energy physics community has made in MINOS, and the fact that, together with MiniBooNE, it will be the center of the domestic U. S. accelerator neutrino program during the next 10 years, there is strong motivation for planning upgrades and extensions of this experiment. Several studies have discussed the physics that could be accessed with a higher-intensity conventional neutrino beam, also involving upgrades to the proton intensity, at Fermilab [12]- [19]. Earlier related efforts studied the physics reach of a neutrino factory, including the U.S. studies [20,21] and related studies in Europe and Japan. In the U. S. an effort is also underway to study the physics potential of long-baseline neutrino oscillation experiments using the BNL AGS, upgraded from 0.14 MW to 0.5 MW, with a very large, multi-hundred kton water Cherenkov far detector [21,22].

Here we address research and development for a second far detector using the MINOS beam and optimized for the study of $\nu_\mu \to \nu_e$ oscillations. In vacuum (e.g. [13,14])

$$\begin{aligned} P(\nu_\mu \to \nu_e) &= 2\sin(2\theta_{13}) s_{23} c_{13} s_{12} (s_{12} s_{23} s_{13} - c_{12} c_{23} c_\delta) \sin^2\phi_{32} \\ &+ 2\sin(2\theta_{13}) s_{23} c_{13} c_{12} (c_{12} s_{23} s_{13} + s_{12} c_{23} c_\delta) \sin^2\phi_{31} \\ &- 2\sin(2\theta_{12}) c^2_{13} \Big[s_{12} c_{12} (s^2_{13} s^2_{23} - c^2_{23}) + s_{13} s_{23} c_{23} (s^2_{12} - c^2_{12}) c_\delta \Big] \sin^2\phi_{21} \\ &+ \frac{1}{2} \sin(2\theta_{12}) \sin(2\theta_{13}) \sin(2\theta_{23}) c_{13} s_\delta \Big[\sin\phi_{32} \cos\phi_{32} \\ &- \sin\phi_{31} \cos\phi_{31} + \sin\phi_{21} \cos\phi_{21} \Big], \end{aligned} \tag{3.3}$$

while the same expression applies for $P(\bar{\nu}_\mu \to \bar{\nu}_e)$ after performing $\delta \to -\delta$.

In the limit $\Delta m^2_{12} \to 0$ (this applies if the solution to the solar neutrino puzzle is in the LOW region),

$$P(\nu_\mu \to \nu_e) = \sin^2(2\theta_{13}) \sin^2\theta_{23} \sin^2\phi_{32}, \tag{3.4}$$

in vacuum. Hence, since one knows $\sin^2\theta_{23}$ and $|\Delta m^2_{32}|$ moderately well from the atmospheric neutrino data (and these determinations will become more accurate with MINOS), it follows that a measurement of, or search for, $\nu_\mu \to \nu_e$ will immediately yield the value of, or a limit on, $\sin^2(2\theta_{13})$.

In general, however, (this applies if the solution to the solar neutrino puzzle is in the LMA region, which is favored by the current solar neutrino data) several of the terms in Eq. (3.3)

can be of the same order of magnitude. In this case, a signal for $\nu_\mu \to \nu_e$ (or lack thereof) does not easily translate into a clean measurement of (or upper bound on) θ_{13}, unless all other parameters are precisely known. It should also be noted that, if matter effects [23] are important, the survival probabilities will also depend on another observable, namely the neutrino mass hierarchy, which we choose to parametrize by the sign of Δm^2_{23}. (Whether matter effects are visible depends on the energy of the neutrino beam and on the baseline length; they tend to be more important for higher energies and longer pathlengths.) This ultimately implies that, in order to determine or constrain θ_{13}, it is necessary also to determine several other neutrino oscillation parameters, including the neutrino mass hierarchy and the CP-odd phase δ. This can only be achieved by comparing different channels (neutrino and antineutrino oscillations) and/or different neutrino beams and different baselines.

Turning the picture around, the study of the subleading $\nu_\mu \to \nu_e$ transition untimately enables (indeed, requires) one to explore leptonic CP violation. This leptonic CP violation involves the phase δ (and two Majorana phases which cannot be directly probed with neutrino oscillations) and is measured by the rephasing-invariant quantity [26] determined via the product $Im(U_{ij}U_{kn}U^*_{in}U^*_{kj})$,

$$J = \frac{1}{8}\sin(2\theta_{12})\sin(2\theta_{23})\sin(2\theta_{13})\cos\theta_{13}\sin\delta \tag{3.5}$$

Because one knows that $\sin^2 2\theta_{23} \simeq 1$ from the atmospheric data and $\sin^2 2\theta_{12} \simeq 0.8$ in the LMA fit to the solar data, it follows that J in the leptonic sector may be much larger than its value of few $\times 10^{-5}$ in the quark sector. Furthermore, the values of $|\Delta m^2_{32}|$ and Δm^2_{21} are such that the corresponding three neutrino mass eigenstates are sufficiently large and nondegenerate so as to allow possible experimental exploration of leptonic CP violation in long-baseline neutrino oscillation experiments. It should be noted that comparison of neutrino and antineutrino oscillations also allows one to probe violation of CPT [27].

The MINOS far detector is comprised of magnetized iron slabs with plastic scintillator and is a course-grained sampling calorimeter with muon ID and momentum measurement. It can provide some modest sensitivity to $\nu_\mu \to \nu_e$ oscillations but is not optimized for this. A major background is neutral current π^0 production, since it is difficult to distinguish the shower produced by the π^0 from the shower produced by an electron. The search for $\nu_\mu \to \nu_e$ oscillations motivates planning and constructing a second, fine-grained, far detector which would take advantage of the NuMI beam. To reduce the high-energy part of the neutrino flux and thereby reduce backgrounds to this search due to neutral current π^0 production, the use an off-axis position for this second far detector becomes ideal.

The physics goals of this program would thus include the following:

- Further measurement of ν_μ disappearance and determination of $|\Delta m^2_{32}|$ and $\sin^2 2\theta_{23}$ to higher accuracy.

- Search for $\nu_\mu \to \nu_e$. In order for this Fermilab-based program to be worthwhile, it should be designed to be as sensitive as the projections stated for the JHF-SK program, which are to be sensitive to values of $\sin^2\theta_{13}$ down to 0.0015 [11].

- Given that some interesting baselines are quite long, of order 10^3 km (assuming that the typical neutrino energies explored will be above 1 GeV), the study of matter effects (which is possible if one runs both neutrino and antineutrino beams) should allow the determination of the neutrino mass hierarchy. Such a measurement cannot be performed by the JHF-SK experiment in Japan, as currently envisioned [11]. It should be noted that this is obtainable even of the solution to the solar neutrino puzzle is not in the LMA region [18].
- With sufficiently accurate knowledge of Δm^2_{32}, $\sin^2 2\theta_{23}$, Δm^2_{21}, and $\sin^2 2\theta_{12}$, it may be possible to obtain significant information on the CP-violating phase δ. This will require analysis of certain parameter ambiguities [28] and of matter effects [23]- [25], and the sensitivity will depend on the pathlength(s) of the experiment.

Given this possible physics potential, there is more than enough motivation to carry out an R&D study of various promising types of detectors and simulations of their response. A study group has been meeting at Fermilab for the past year to discuss this. Recently one report was submitted [29]. We believe that it is clear that this work should be pursued with further R&D.

IV. DETECTOR ISSUES AND COMPARISON

A. Detector Requirements for θ_{13}

1. Neutral Current Rejection in a superbeam

2. Intrinsic ν_e Rejection in a superbeam

It's the Energy resolution!

3. Charge identification in a neutrino factory

B. Operation at the Surface

C. Expandability

D. Cost comparisons

E. Fiducial vs Total Mass

V. TOTAL ABSORPTION DETECTORS

A. Liquid Argon Detectors

(** Kirk McDonald)

B. R& D Issues for Liquid Argon Detectors

C. Water Cherenkov Detectors

(** Mark Messier)

D. R& D Issues for Water Cherenkov Detectors

E. Water Rich Detectors

(Scott Menary)

F. R& D Issues for RICH Detectors

G. KamLAND-like Detectors

H. R& D Issues for KamLAND-like Detectors

VI. SAMPLING DETECTORS

A. Absorber Issues

1. steel

(** Jeff Nelson)

2. plastic

(** Jeff Nelson)

3. water

(** Jeff Nelson)

4. cheap low Z material

Coal, walnuts, cracked corn...

B. Solid Scintillator Detectors

(Mayda Velasco)

C. R& D Issues for Solid Scintillator Detectors

D. Liquid Scintillator Detectors

(Ken Heller)

E. R& D Issues for Liquid Scintillator Detectors

F. RPC/gas Detectors

(Peter Shanahan)

G. R& D Issues for RPC/gas Detectors

H. Emulsion Detectors

I. R& D Issues for Emulsion Detectors

VII. OTHER R& D ISSUES

A. cross sections

(** Kevin McFarland)

B. pion yields

(**Mark Messier)

C. targetry

(** Mikhail Kostin, Nikolai Mokhov)

The target will remain the most critical device in the NuMI beamline after upgrade of the Fermilab accelerator complex with a Proton Driver. The target must be able to survive a 2MW proton beam with some safety margin. A good target for a neutrino superbeam facility would satisfy the following conditions: it survives one spill; a steady state temperature must not exceed a temperature stress limit; the target life time is greater than 6 months; in the case of multiple choice for a target candidate, the optimal target is the one that provides the highest π^+ yield in the energy interval of interest. The first three clauses are quite obvious. The last one is driven by the physics case. An off-axis neutrino beam of a required energy of ≈ 3 GeV will be formed by secondary pions with energy in the 6–14 GeV interval. Not all the pions of such energy will contribute to neutrino beam. A beamline focusing system acts differently on pions with different transverse momentum. Moreover, the focusing system itself

would not be necessarily same for different targets. Therefore we use a simplified approach for these studies. An integrated over p_T pion flux is used for the target optimization.

1. What survives one spill ?

A number of commonly used materials was considered for a target. The target was simulated with the MARS14 code [30]. We assumed that a 120 GeV proton beam hits a rod target with a length of two interaction lengths. For the first trial, the beam was assumed to be a Gaussian with $\sigma_x = \sigma_y = 1$ mm (approximately NuMI parameters). The target radius R_T was optimized for the maximal pion yield scanning the radius of target with a step of 0.5 mm starting from 2.5 mm (see Table I). In order to achieve a power of 2 MW, the nominal NuMI beam intensity is rescaled by a factor of 5 that corresponds to $2{\times}10^{14}$ protons per spill. We also assumed that the Main Injector repetition period of 1.9 s does not change.

Calculated peak energy deposition densities (ED) on a beam axis are shown in Table I for C through Hg targets. For the beam conditions described above all the materials experience a significant thermal shock. The stress limits known for graphite, nickel and inconel are about 1000 J/g. The limit for copper is about 600 J/g. As one can see from the table, none of the solid materials can survive such conditions.

Despite the fact that the above conditions are not operable for the solid materials, it is interesting to notice that the pion yield in the defined energy interval does not vary significantly with the target material (Table I). Fig. 1 shows the pion yield versus pion energy for graphite and mercury. Much more soft pions are produced in a mercury target. But what is important, the yield is about the same in the energy region of interest. Pion spectra for the other materials studied behave similarly.

The most obvious idea of stress reduction is to increase the beam transverse spot size. In the study below, both the beam spot size $\sigma = \sigma_x = \sigma_y$ and target radius R_T are varied. For a graphite target the pion yield as a function of R_T/σ is shown in Fig. 2 for different σ. As one can see the variation of the maximal yeild for different σ does not exceed 7%. This is due to the fact that pions leave the target at much larger angle than a specific angle at which the target collimates the pions, that is $\mathrm{atan}(R_T/\lambda_I) \approx 1^\circ$ (Fig. 3). Energy deposition in the hottest cell of target is acceptable at $\sigma > 1.5$ mm (Fig. 4). For example, for σ=3 mm and target radius R_T=9 mm the peak energy deposition is 310 J/g that is well below the limit. Thus the beam spot size and target radius for graphite can be substantially increased compared to the NuMI parameters without significant loss of the yield.

Material	Peak ED (J/g)	π^+yield (N/POT)	optimal R_T (mm)
Graphite	1581 ± 18	0.754 ± 0.007	5.0
Nickel	6520 ± 251	0.684 ± 0.006	2.5
Inconel	6011 ± 259	0.699 ± 0.006	3.0
Copper	6084 ± 216	0.690 ± 0.006	2.5
Indium	5248 ± 149	0.752 ± 0.006	3.0
Mercury	10064 ± 293	0.715 ± 0.006	3.0

TABLE I. Density of peak energy deposition and pion yield in the 6–14 GeV interval for various targets. Also shown are the optimal target radii R_T for σ=1 mm.

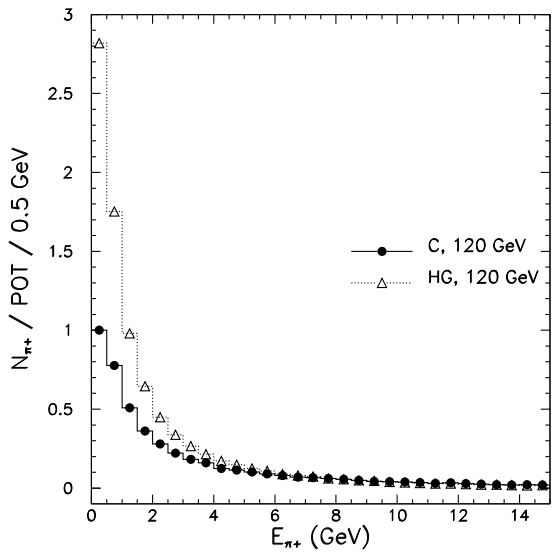

FIG. 1. Pion yield versus pion energy. The distributions are normalized per the number of protons on target (POT).

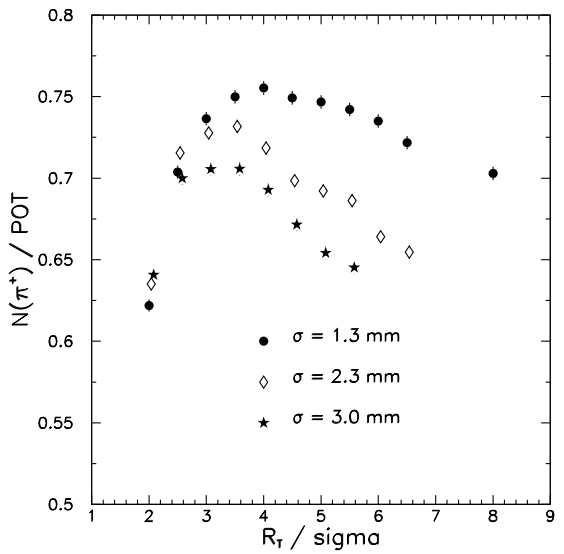

FIG. 2. Number of π^+ coming from a graphite target in the interval 6–14 GeV against the value of target radius over beam sigma. Shown are dependencies for different beam RMSs.

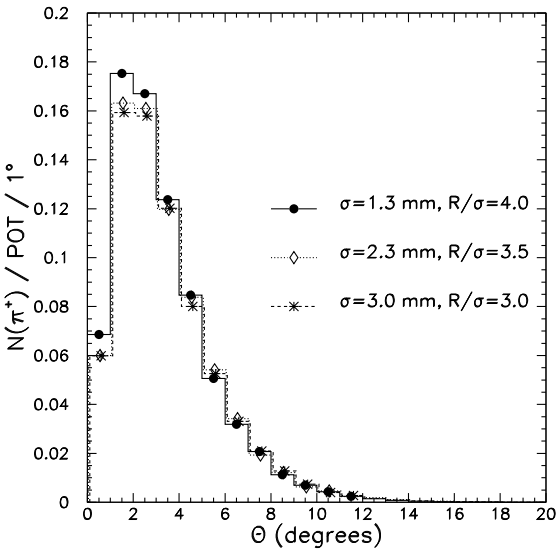

FIG. 3. Angular distributions for pions coming off a graphite target. θ is an angle between the target axis and pion direction.

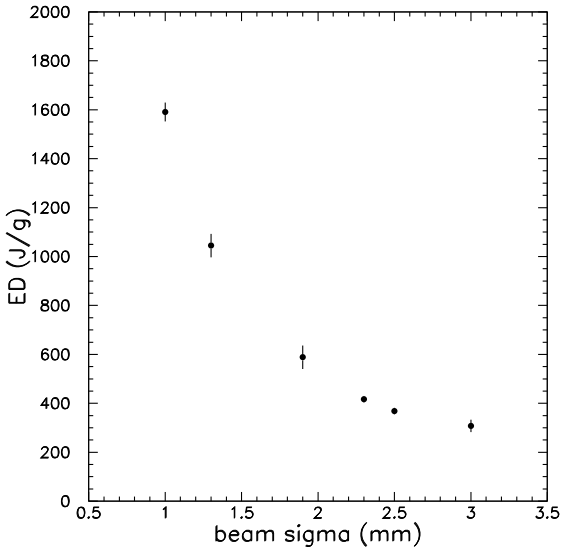

FIG. 4. Energy deposition in the hottest cell of a graphite target versus beam spot size.

The same idea does not work well for solid dense materials. An attempt to bring the energy deposition safely below the limit by increasing σ and R_T results in a substantial reduction of the pion yield. For example, if one increases the beam σ up to 12.5 mm keeping the ratio to be optimal $R_T/\sigma = 2.5$, the pion yield from an inconel target reduces down to 0.43 pions per proton that is much smaller than the yield of about 0.71 from an optimal graphite target. The density of peak energy deposition is 1250 J/g in this case that is still

above the limit.

The studies performed show that graphite is the most convenient material for a FNAL neutrino superbeam facility. Indeed, the dense solid materials do not provide enough of pion flux at the acceptable beam and target radii. The use of light materials with large interaction lengths such as Li and Na will lead to a too long target, making focusing of secondaries problematic. A mercury jet target seems to be too complex, expensive and hazardous device and at the same time it does not provide any advantages over a graphite target for the given experimental conditions.

2. Target life-time

One of the factors limiting the target life-time is radiation damage. The life-time determined here corresponds to the time when 5 dpa (displacements per atom) occur in the hottest cell of the target. The atoms are displaced due to interactions with hadrons with kinetic energy of >0.1 MeV. The 5 dpa limit corresponds to the integrated hadron flux of about 5×10^{22} cm^{-2}. From the MARS simulations we have found that for the beam σ=3mm and graphite target radius R_T=9mm the limit of 5 dpa is reached within 5 years and 8 months assuming 10 months of operation per year at the full intensity.

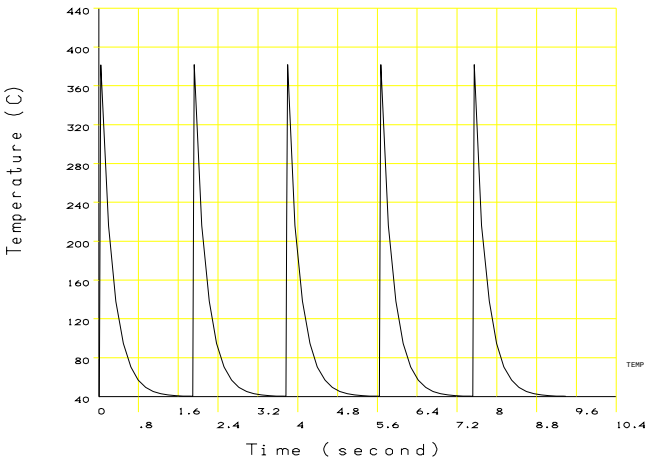

FIG. 5. Temperature evolution in the hottest cell of a graphite target with 1.9 s repetition rate.

3. Temperature buildup

The temperature evolution in a graphite target has been investigated with the ANSYS code [31]. An ED distribution in a target with R_T=9mm was simulated with MARS. The

beam σ was chosen to be 3mm. The temperature rise for the target elements was estimated from the ED distribution and was assumed to be instant. The temperature rise was applied to the target every 1.9 sec. A simplified cooling system was used in this simulation. The heat excess was brought away from the target by water with constant temperature of 40° C running around the outer cylindrical surface of the target. As Fig. 5 shows, the temperature in the hottest cell oscillates between 40° C and 380° C without any buildup. The tensile stress obtained from the simulation is about 20 MPa at the tensile strength for graphite of about 90 MPa.

4. Conclusions

A graphite target represents a simple and cheap solution for the FNAL neutrino superbeam facility. Such a target satisfies all the requirements applied: it survives one spill; radiation damage does not constrain the life-time significantly; there is no temperature buildup in target; pion yield is quite high.

D. Proton Intensity

Doug Michael?

VIII. SUMMARY AND CONCLUSIONS

---

[1] Recent solar data is in S. Fukuda, et al. Phys. Rev. Lett. **86**, 5651 (2001), S. Fukuda et al., *ibid*, 5656 (2001) (SuperKamiokande) and Q.R. Ahmad et al., Phys. Rev. Lett. **87**, 071301 (2001), nucl-ex/0204008, nucl-ex/0204009 (SNO). The Homestake, Kamiokande, GALLEX, and SAGE experiments provided earlier data.

[2] See, for example, Q.R. Ahmad et al. in [1].

[3] Y. Fukuda et al., Phys. Lett. **B433**, 9 (1998); Phys. Rev. Lett. **81**,1562 (1998); *ibid.*, **82**, 2644 (1999); Phys. Lett. **B467**, 185 (1999) (SuperK). Other data is from the Kamiokande, IMB, Soudan-2, and MACRO experiments; see, e.g., talks at Neutrino-2000, Neutrino-2002.

[4] S. H. Ahn et al., Phys. Lett. **B511**, 178 (2001); J. Hill, talk at the NOON Conf. (Dec., 2001).

[5] M. Apollonio et al., Phys. Lett. **B420**, 397 (1998); Phys. Lett. **B466**, 415 (1999).

[6] C. Athanassopoulous et al., Phys. Rev. Lett. **77**, 3082 (1996); Phys. Rev. Lett. **81**, 1774 (1998); A. Aguilar et al., hep-ex/0104049.

[7] M. Steidl for the KARMEN Collaboration, Nucl. Phys. Proc. Suppl. **100**, 188 (2001).

[8] See http://www-numi.fnal.gov/ .

[9] See http://www-boone.fnal.gov/ .

[10] See http://proj-cngs.web.cern.ch/proj-cngs/.

[11] See http://neutrino.kek.jp/jhfnu, in particular, Y. Itoh et al., "Letter of Intent: A Long Baseline Neutrino Oscillation Experiment using the JHF 50 GeV Proton Synchrotron and the Super-Kamiokande Detector" (Feb. 2000); Y. Itoh et al, "The JHF-Kamioka Neutrino Project", hep-ex/0106019.
[12] V. Barger et al. (Fermilab Superbeam Working Group), Nov., 2000, hep-ph/0103052.
[13] V. Barger, S. Geer, R. Raja, and K. Whisnant, Phys. Rev. **D63**, 113011 (2001).
[14] I. Mocioiu and R. Shrock, JHEP 0111, 050 (28 pages) (2001).
[15] UNO Protocollaboration and Theoretical Advisory Committee, 'Physics Potential and Feasibility of UNO", UNO Snowmass 2001 White Paper, June, 2001.
[16] Snowmass E1 Working Group (T. Adams et al.), E1 Working Group Summary: Neutrino Factories and Muon Colliders, hep-ph/0111030.
[17] W. Chou, ed. "Proton Driver Design Study", Fermilab-TM-2136 (2001).
[18] G. Barenboim et al., hep-ph/0204208.
[19] G. Barenboim, A. de Gouvea, T. Dombeck, N. Grossman, D. Harris, D. Michael, M. Szleper, M. Velasco, and S. Werkema, hep-ex/0206025.
[20] C. Albright et al. (Fermilab Neutrino Factory Physics Working Group), "Physics at a Neutrino Factory", Apr. 2000, hep-ph/hep-ex/0008064. (See also the companion machine study "Feasibility Study of a Neutrino Factory Based on a Muon Storage Ring", by the Fermilab Neutrino Factory Feasibility Study Working Group, N. Holtkamp, et al.)
[21] Muon Collider and Neutrino Factory Collaboration, "Neutrino Factory Feasibility Study II" (May 2001), available at http://www.cap.bnl.gov/mumu.
[22] e.g., K. McDonald and R. Shrock, talks at Snowmass 2001, June, 2001; W. Marciano, hep-ph/0108181; A. Mann et al. (3M Protocollaboration), "Megaton Modular Multi-Purpose Neutrino Detector" (Nov. 2001); D. Beavis et al., Neutrino Oscillation Experiments for Precise Measurements of Oscillation Parameters and Search for Muon-Neutrino to Electron Neutrino Appearance and CP Violation: Letter of Intent to Brookhaven National Laboratory", hep-ex/0205040.
[23] L. Wolfenstein, Phys. Rev. **D17**, 2369 (1978); S. P. Mikheyev and A. Smirnov, Yad. Fiz. **42**, 1441 (1985) [Sov.J. Nucl. Phys. **42**, 913 (1986)], Nuovo Cim., **C9**, 17 (1986).
[24] V. Barger, K. Whisnant, S. Pakvasa, and R. J. N. Phillips, Phys. Rev. **D22**, 2718 (1980); P. Krastev, Nuovo Cimento **103A**, 361 (1990); R. H. Bernstein and S. J. Parke, Phys. Rev. **D44**, 2069 (1991); De Rujula, M. B. Gavela, and P. Hernandez, Nucl. Phys. **B547**, 21 (1999); P. Lipari, Phys.Rev. **D61**, 113004 (2000) S. Dutta, R. Gandhi, and B. Mukhopadhyaya, Eur.Phys.J. **C18**, 405 (2000); V. Barger, S. Geer, K. Whisnant, Phys.Rev. **D61**, 053004 (2000); D. Dooling, C. Giunti, K. Kang, C. W. Kim,Phys.Rev. **D61**,073011 (2000); A. Bueno, M. Campanelli, A. Rubbia, Nucl.Phys. **B573**, 27 (2000); V. Barger, S. Geer, R. Raja, K. Whisnant, Phys.Rev. **D62**, 013004 (2000); M. Freund, M. Linder, S.T. Petcov, A. Romanino, Nucl.Phys. **B578**, 27 (2000); I. Mocioiu and R. Shrock, AIP Conf.Proc. **533**, 74 (2000) (NNN99); I. Mocioiu and R. Shrock, Phys.Rev. **D62**, 053017 (2000); V. Barger, S. Geer, R. Raja, K. Whisnant, Phys.Rev. **D62**, 073002 (2000); A. Cervera, A. Donini, M.B. Gavela, J. Gomez Cadenas, P. Hernandez, O. Mena, and S. Rigolin, Nucl.Phys. **B579**, 17 (2000), Erratum-ibid. **B593**, 731 (2001); M. Freund, P. Huber, M. Lindner, Nucl.Phys. **B585**, 105 (2000); V. Barger, S. Geer, R. Raja, K. Whisnant, Phys.Lett. **B485**, 379 (2000); Z.-Z. Xing, Phys. Lett. **487**, 327 (2000); Phys. Rev.

D63, 073012 (2000); A. Bueno, M. Campanelli, A. Rubbia, Nucl.Phys. **B589**, 577 (2000); P. Fishbane, Phys. Rev. **D62**, 093009 (2000); P. Fishbane and P. Kaus, Phys. Lett. **B506**, 275 (2001); P. Fishbane and S. Gasiorowicz, hep-ph/0012230; V. Barger, S. Geer, R. Raja, K. Whisnant, Phys.Rev. **D63**, 033002 (2001); M. Freund, P. Huber, M. Lindner, hep-ph/0105071. E. Akhmedov, A. Dighe, P. Lipari, A. Smirnov, Nucl. Phys. **B542**, 3 (1999); E. Akhmedov, Nucl.Phys. **B538**, 25 (1999); E. Akhmedov, hep-ph/0001264; E. Akhmedov, P. Huber, M. Lindner, and T. Ohlsson, hep-ph/0105029; J. Arafune, J. Sato, Phys.Rev. **D55**, 1653 (1997); H. Minakata, H. Nunokawa, Phys.Rev. **D57**, 4403 (1998); M. Koike, J. Sato, hep-ph/9707203, Phys.Rev. **D62**, 073006 (2000).

[25] A. Romanino, Nucl.Phys. **B574** 675 (2000); S.M. Bilenky, C. Giunti, W.Grimus, Phys.Rev. **D58**, 033001 (1998); K. Dick, M. Freund, M. Lindner, A. Romanino, Nucl. Phys. **B562**, 29 (1999); M. Tanimoto, Phys. Lett. **B462**, 115 (1999); A. Donini, M.B. Gavela, P. Hernandez, S. Rigolin, Nucl.Phys. **B574**, 23 (2000); M. Koike, J. Sato, Phys.Rev. **D61**, 073012 (2000), Erratum-ibid. **D62**, 079903 (2000); S. J. Parke, T. J. Weiler, Phys.Lett. **B501**, 106 (2001); T. Miura, E. Takasugi, Y. Kuno, and M. Yoshimura, Phys. Rev. **D64**, 013002 (2001); M. Koike, T. Ota, J. Sato, hep-ph/0011387; P. Lipari. hep-ph/0102046.

[26] C. Jarlskog, Z. Phys. **C29**, 491 (1985); Phys. Rev. **D35**, 1685) (1987).

[27] V. Barger, S. Pakvasa, T. Weiler, and K. Whisnant, Phys. Rev. Lett. **85**, 5055 (2000); H. Murayama and T. Yanagida, Phys. Lett. **B520**, 263 (2001); G. Barenboim, L. Borissov, J. Lykken and A. Smirnov, hep-ph/0108199; G. Barenboim, L. Borissov, and J. Lykken, Phys. Lett. **B534**, 106 (2002); G. Barenboim, J. Beacom, L. Borissov, and B. Kayser, Phys. Lett. **B537**, 227 (2002); I. Mocioiu and M. Pospelov, Phys. Lett. **B534**, 114 (2002); A. Strumia, hep-ph/0201134.

[28] e.g., V. Barger, D. Marfatia, and K. Whisnant, hep-ph/0206038.

[29] D. Ayres et al. (A. Para, contact person), "Letter of Intent to Build an Off-Axis Detector to Study $\nu_\mu \to \nu_e$ Oscillations with the NUMI Neutrino Beam", June, 2002.

[30] N. V. Mokhov, "The MARS Monte Carlo", Fermilab FN-628 (1995); N. V. Mokhov and O. E. Krivosheev, "MARS Code Status", Fermilab-Conf-00/181 (2000); http://www-ap.fnal.gov/MARS/.

[31] "ANSYS (rev.5.1)", Swanson Analysis System, Inc., SASI/DN-P511:51, Houston (1994).